Journal of Catalysis 260 (2008) 134–140

Contents lists available at ScienceDirect

Journal of Catalysis

www.elsevier.com/locate/jcat

Direct splitting of H_2S into H_2 and S on CdS-based photocatalyst under visible light irradiation

Guijun Ma, Hongjian Yan, Jingying Shi, Xu Zong, Zhibing Lei, Can Li *

State Key Laboratory of Catalysis, Dalian Institute of Chemical Physics, Chinese Academy of Sciences, Dalian 116023, China

ARTICLE INFO

Article history:
Received 15 July 2008
Revised 27 August 2008
Accepted 15 September 2008
Available online 16 October 2008

Keywords:
Cadmium sulfide
Ethanolamine
Polysulfide
Hydrogen production
Hydrogen sulfide conversion
Photocatalysis
Electrochemistry

ABSTRACT

The conversion of H_2S into H_2 and S ($H_2S \rightarrow H_2 + S$) is beneficial from both environmental and energy standpoints. Here we report that H_2S can be splitted stoichiometrically into hydrogen and sulfur on CdS-based photocatalysts under visible light irradiation using ethanolamine as a H_2S solvent and reaction media at room temperature. Raman spectra showed that the produced sulfur existed as S_4^{2-} and S_6^{2-} after photocatalytic reaction. The hydroxyls of the reaction media were found to be crucial for the hydrogen production, and the rate-determining step (RDS) of photocatalytic splitting H_2S in diethanolamine is discussed. Electrochemical evaluation showed that the potential of H_2S splitting in ethanolamine was greatly lowered and the photogenerated electrons could be fully used to reduce protons for hydrogen production. A free-radical-related one-electron electrochemical oxidation process on platinum electrode is suggested. This work demonstrates the possibility of the direct splitting H_2S into S and H_2 via photocatalysis.

1. Introduction

Hydrogen sulfide (H_2S) is a toxic chemical emitted in large quantities from both natural sources and industrial processes [1–4]. An increasing source of H_2S is produced in large quantity from chemical industry such as natural gas utilization, hydrodesulfurization of crude oil and coal chemistry [3,4]. Even with trace amount, H_2S has serious poisoning effect on noble metal catalysts used in many industrial processes, including hydrogenation, ammonia synthesis, and fuel cells [5,6]. Most of the current industrial technology for removing H_2S is an absorption/stripping system using aqueous solutions of ethanolamines, followed by a Claus process to decompose H_2S into water and sulfur [$H_2S + (1/2)O_2 \rightarrow H_2O + S$] [7]. But this is not an economically viable process, due to the high cost of the chemical process and the process actually results further environmental problem [8]. More importantly, the hydrogen (a highly in-demand raw chemical and energy source) potentially stored in H_2S is not reclaimed in the Claus process [8,9].

Various strategies for converting H_2S into hydrogen and sulfur to resolve the environmental problems and produce hydrogen have been proposed. For example, the thermal decomposition of H_2S into H_2 and S has been well investigated [9,10]. But the equilibrium conversion is quite low even at high temperatures, because the complete splitting reaction of H_2S is thermodynamically unfavorable ($\Delta G^0 = 33$ kJ/mol); therefore, thermal and other conventional methods to directly convert H_2S require additional energy [9,10]. Scientifically, the direct decomposition of H_2S into H_2 and S is a very interesting chemical reaction, involving a series of important chemical processes, including photocatalytic splitting of H_2O into H_2 and O_2 [11].

Growing concerns about the environment and resource utilization have pushed the research for novel technologies to convert H_2S to S and H_2 using solar energy [11,12]. Recovery of both hydrogen and sulfur from H_2S through environmentally friendly photocatalytic technology is an ideal alternative to the Claus process. The indirect conversion of H_2S with photocatalysis has been extensively investigated. In this process, H_2S is dissolved in a basic aqueous solution, such as NaOH, to produce sulfide ions (S^{2-} and/or HS^-), and then the sulfide ions are used as sacrificial agents in photocatalytic hydrogen production reaction from water [13–18]. Unfortunately, additional reducing agents, such as sulfite (SO_3^{2-}) or hypophosphite ($H_2PO_2^-$), must be used together with the sulfide ions to maintain the catalytic activity while producing various byproducts (e.g., $S_2O_3^{2-}$, SO_4^{2-}, $S_2O_6^{2-}$) in aqueous solution instead of elemental sulfur. The diluted solution with the sulfur oxysalts ($S_2O_3^{2-}$, SO_4^{2-}, $S_2O_6^{2-}$) is a major source of pollutants from chemical industry; obviously, separating and purifying such diluted byproducts is more costly and difficult than treating H_2S by the conventional Claus process.

Therefore, a direct splitting of H_2S to produce H_2 and S using solar energy is the most promising desirable process to solve the environmental problems and produce clean energy, H_2. Here we

---

* Corresponding author. Fax: +86 411 84694447.
E-mail address: canli@dicp.ac.cn (C. Li).

0021-9517/$ – see front matter © 2008 Elsevier Inc. All rights reserved.
doi:10.1016/j.jcat.2008.09.017

found that H_2S can be stoichiometrically converted to H_2 and S in ethanolamine solvent under visible light irradiation, and that the quantum efficiency for the hydrogen production can be as high as 30% for CdS-based semiconductor materials loaded with noble metals as co-catalysts.

2. Experimental

2.1. Preparation and characterization of CdS

Highly crystalline CdS nanoparticles were prepared by a precipitation-hydrothermal process. All of the reagents were analytical grade and used without further purification. In a typical preparation procedure, $Cd(CH_3COO)_2 \cdot 2H_2O$ was dissolved in water with a concentration of $0.15\ mol\,L^{-1}$ (M) and precipitated by aqueous Na_2S solution. The yellow amorphous CdS was washed with copious deionized water, followed by hydrothermal crystallization at 200 °C for 3 days in a Teflon-lined stainless steel autoclave. The CdS powder was collected by filtration and washed several times with water and ethanol. After drying at 80 °C in a vacuum, the final yellow powder was obtained.

Transmission electron microscopy (TEM) (JEOL JEM-2000EX, 120 kV) images of the catalyst sample demonstrated a mean crystalline size of CdS particles of about 50 nm. X-ray diffraction (XRD) (Rigaku D/max-2500 diffractometer, Cu$K\alpha$, 40 kV, 100 mA) and high-resolution TEM (HRTEM) showed that the prepared CdS was well crystallized with a pure hexagonal wurtzite structure.

2.2. Loading of M, Pt–M, MS, and Pt–MS on CdS

$H_2PtCl_6 \cdot 6H_2O$(99.99%) and $RuCl_3 \cdot xH_2O$ were purchased from China Medicine Shanghai Chemical Reagent Corp. $PdCl_2 \cdot 2H_2O$ and $RhCl_3 \cdot xH_2O$ were purchased from China Beijing Chemical Reagent Corp. The aqueous solution of noble metal compound was prepared from deionized water. All chemicals were used as received.

Noble metals (M and Pt–M) were loaded onto CdS as a co-catalyst by in situ photochemical deposition [15–19]. Typically, the prepared CdS powder (0.5 g) was dispersed in aqueous acetic solution (150 ml 0.1 M), followed by the addition of appropriate amount of noble metal compound solutions. Then the mixture was irradiated under visible light (300 W Xe lamp, $\lambda > 420$ nm) in vacuum for 0.5 h to photoreduce the noble metal on the CdS surface. The reacted solution was filtrated and washed with deionized water to get an M/CdS (Pt–M/CdS) photocatalyst. Noble metal sulfide (MS or Pt–MS) was loaded on CdS by precipitation method. Typically, the CdS (Pt/PdS) was dispersed in aqueous Na_2S solution (150 ml 0.3 M), followed by the slow addition of the corresponding noble metal compound solution. Then, similar to the aforementioned process, the solution was irradiated in vacuum and filtrated to produce MS/CdS (Pt–MS/CdS).

2.3. Photocatalytic reactions

Photocatalytic reaction solutions were prepared by dissolving H_2S gas (99.9%) in different amine solvents that had been previously dehydrated with molecular sieves (5-Å). The concentration of sulfide ions in solvent was determined by the titration method [20]. The H_2S-amine solution was mixed with an excess of acidic I_2–KI solution (0.05 M). The excess iodine was back-titrated with $Na_2S_2O_3$ solution (0.05 M), using starch as an indicator:

$$C + H_2S = C_{I_2-KI} \times V_{I_2-KI}/V_{H_2S}.$$

Photoactivities of the samples were examined in a closed gas circulation and evacuation system [15–19]. The evolved amounts of H_2 were analyzed by online gas chromatography (TCD, molecular sieve 5-Å column, and Ar carrier). The M/CdS photocatalyst was dispersed in a Pyrex reaction cell containing 100 mL of H_2S-amine solutions. A thermostatted water jacket was set around the reaction cell to control the reaction solution at a prespecified temperature. A 300-W Xe lamp equipped with an optical cutoff filter ($\lambda > 420$ nm) was used as the light source. A shutter window filled with water was placed between the Xe lamp and the reaction cell to remove infrared light illumination.

2.4. Raman spectra

Raman scattering spectra were recorded in back-scattering geometry on an Acton Raman spectrometer equipped with a liquid nitrogen-cooled CCD detector at a resolution of 4 cm^{-1}. A 532-nm semiconductor laser was used as the excitation source, and the laser power at the sample was set as 60 mW. All experiments were performed with a quartz tube at room temperature.

2.5. Electrochemical experiments

A typical three-electrode electrochemical system was used for linear sweep voltammetry measurements. A platinum plate was used as the working electrode with surface area of around 6 cm^2, with another platinum plate with a much larger surface area used as the counter-electrode and an SCE used as the reference electrode. The desired solid Na_2SO_4 was added to the H_2S–DEA or Na_2S–NaOH solution up to a concentration of 0.2 M to function as a supporting electrolyte. The scan rate was 50 mV/s, and all measurements were carried out on an EG&G 2273A potentiostat/galvanostat at room temperature. The electrolyte was kept under continuous magnetic stirring during the measurements.

3. Results and discussion

3.1. Photocatalytic splitting of H_2S in ethanolamines

Fig. 1 shows the photocatalytic H_2 evolution from H_2S splitting on Pt/CdS catalyst in the different ethanolamine solvents used to absorb/dissolve H_2S and also as the reaction media. These ethanolamines—monoethanolamine (MEA), $H_2NCH_2CH_2OH$, diethanolamine (DEA), $HN(CH_2CH_2OH)_2$, and triethanolamine (TEA), $N(CH_2CH_2OH)_3$—are frequently used as absorbents in industry for H_2S absorption [21]. The Pt/CdS photocatalyst showed high activity in hydrogen production under visible light irradiation for all the three ethanolamine solvents dissolved with H_2S. Among the three solvents tested, the highest activity was observed for DEA

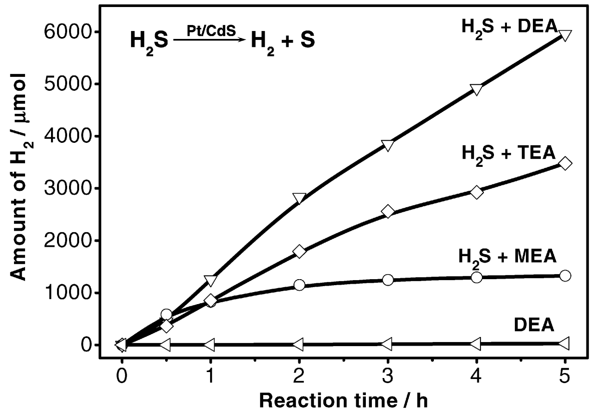

Fig. 1. Photocatalytic H_2 production under visible light irradiation over Pt/CdS (0.20 wt% Pt) in different solutions. DEA: diethanolamine, TEA: triethanolamine, MEA: monoethanolamine. Reaction conditions: volume of solution, 100 ml; concentration of H_2S, 0.30 M; amount of catalyst, 0.025 g; reaction temperature, 30 °C; light source, 300-W Xe lamp with a cutoff filter ($\lambda > 420$ nm).

Table 1
Photocatalytic H_2 production under visible light irradiation over CdS loaded with different co-catalysts in DEA.[a]

Co-catalysts loaded on CdS	None	Ru	Rh	Pd	Pt	Ru_2S_3	Rh_2S_3	PdS	Pt–Ru	Pt–Rh	Pt–Pd	Pt–Ru_2S_3	Pt–Rh_2S_3	Pt–PdS	Pt–Pt
H_2 production (μmol h^{-1})	180	430	440	640	670	570	600	620	660	810	1070	870	710	1460	1190

[a] The amount of noble metals or noble metal sulfides loaded on CdS: 0.10 wt% for single metal; 0.10–0.10 wt% for double metals. Reaction conditions: volume of solution, 100 ml; concentration of H_2S, 0.30 M; amount of catalyst, 0.025 g; reaction temperature, 30 °C; light source, 300-W Xe lamp with a cutoff filter ($\lambda > 420$ nm).

and the average hydrogen production activity can be as high as 25 ml/0.025 g/h. Fig. 1 shows that nearly no hydrogen was produced in the DEA solution with no dissolved H_2S, indicating that the hydrogen was produced only from the splitting of H_2S instead of from the reformation of DEA. No apparent deactivation of the photocatalyst was observed for the hydrogen production from H_2S splitting in the DEA solution.

Naman et al. [22,23] reported the photocatalytic H_2 production from H_2S saturated aqueous solutions of 20% MEA, DEA, and TEA containing suspensions of TiO_2, CdSe, and CdS. For these reaction systems, the highest H_2 production rate was achieved in aqueous MEA solution using the TiO_2 photocatalyst. In aqueous DEA solution, TiO_2 had a slightly higher H_2 production rate than CdS. In nonaqueous ethanolamine solutions, as shown in Fig. 1, the photocatalytic performance of H_2 production was much better in DEA than in MEA. We compared the photocatalytic activity between CdS and TiO_2 (loading no co-catalysts) in the nonaqueous H_2S–DEA solution under UV light irradiation. The results show that the production rate of H_2 on TiO_2 (P25) was only 10% that on CdS. This implies that the photocatalytic splitting of H_2S in nonaqueous ethanolamine solution differed from that in aqueous ethanolamine solution.

Green and Elofson [24] reported the visible light-induced addition of H_2S to hept-1-ene with a major product of heptane-1-thiol (95%) on RuO_2/CdS photocatalyst using nonaqueous acetonitrile as solvent. However, the alkene also intercepted most of the hydrogen ions, resulting a low yield of H_2 (the quantum yield at 447 nm was <1%).

Table 1 displays the photocatalytic activity of hydrogen production from H_2S splitting on CdS loaded with different noble metals and corresponding sulfides as the co-catalysts. (Noble metal sulfides were considered because the noble metals might be partially sulfided in the presence of H_2S.) CdS alone showed low photocatalytic activity in H_2 production. The photocatalyst activity was enhanced significantly by loading a small amount of the co-catalyst on CdS. The hydrogen production activity varied with different noble metals (Pt, Pd, Ru, Rh) and noble metal sulfides (PdS, Rh_2S_3, Ru_2S_3), with the Pt/CdS catalyst showing the greatest activity for the single co-catalyst deposited on CdS. Co-deposition of Pt with other noble metals or their sulfides on CdS demonstrated further enhanced activity in hydrogen production. The activity of Pt–PdS/CdS was even greater than that for the simple sum of Pt/CdS and PdS/CdS, suggesting a synergistic effect between the co-catalysts Pt and PdS [11,17,19]. The promoting effect of loading noble metals on photocatalytic H_2 production activity could be explained by the fact that the two co-catalysts may facilitate separation of the photogenerated electrons and holes on photocatalyst [25,26].

3.2. Characterization of S by Raman spectroscopy

Fig. 2 shows the Raman spectra of H_2S–DEA solution before and after the photocatalytic hydrogen production. The Raman spectra in the range of 300–700 cm^{-1} were similar for DEA and DEA dissolved with H_2S. The Raman bands observed at 350, 380, 450, and 530 cm^{-1} were mainly from DEA. Two additional bands at 390 and 440 cm^{-1} appeared after the photocatalytic reaction of DEA dissolved with H_2S, indicating the formation of sulfur-related products. The Raman bands at 390 and 440 cm^{-1} can be assigned to polysulfide species (S_6^{2-} and S_4^{2-}) [27]. The polysulfide species can be further confirmed through the reaction between sulfide ions with sulfur element in basic solution [28,29]. After the addition of appropriate amount of sulfur powder into fresh H_2S–DEA solution, the sulfur was dissolved in the solution within several minutes. Fig. 3 shows the Raman spectra of the solution recorded with increasing sulfur addition. Two new peaks at around 400 and 440 cm^{-1} became increasingly dominant with an increasing S-to-H_2S ratio. The solution of H_2S–DEA mixed with solid sulfur was similar to the H_2S–DEA solution after the photocatalytic reaction.

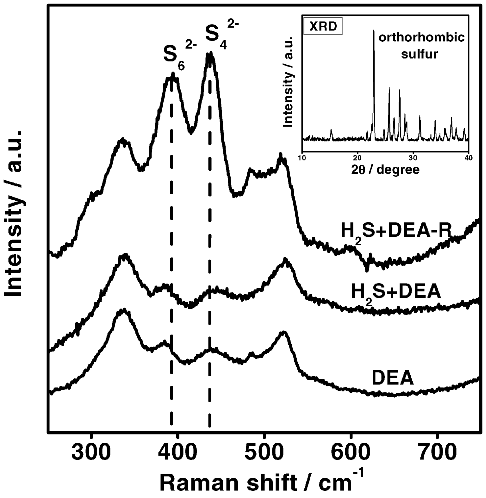

Fig. 2. Raman spectra of DEA and H_2S + DEA before and after photocatalytic reaction, with the excitation line at 532 nm. The inset shows the powder X-ray diffraction (XRD) patterns of the produced sulfur in H_2S + DEA after the photocatalytic reaction. Reaction conditions: volume of solution, 100 ml; concentration of H_2S, 1.60 M; amount of catalyst, 0.025 g Pt (0.2 wt%)/CdS; reaction temperature, 50 °C; light source, 300-W Xe lamp with a cutoff filter ($\lambda > 420$ nm).

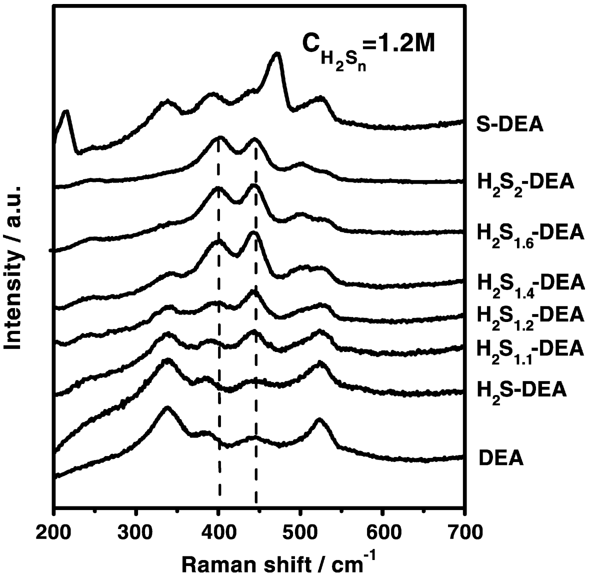

Fig. 3. Raman spectra of DEA, H_2S–DEA and H_2S–DEA with adding of solid sulfur powder into it, recorded at room temperature, with the 532-nm excitation line.

Table 2
Photocatalytic production of H_2 and S from H_2S in DEA under visible light irradiation.[a]

Amount of the products	Runs of the reaction			
	1[b]	2[b]	3[b]	4[c]
H_2 (mmol)	15.5	11.3	11.2	33
S (mmol)	15.1	11.0	10.8	32.5

[a] Reaction conditions: volume of solution, 100 ml; amount of catalyst, 0.025 g; light source, 300-W Xe lamp with a cutoff filter ($\lambda > 420$ nm).

[b] Concentration of H_2S 0.30 M.

[c] Concentration of H_2S 1.60 M.

Table 3
Photocatalytic H_2 production under visible light irradiation over Pt/CdS (0.20 wt% Pt) in different solutions.[a]

Reaction solutions	DEA + H_2S	DA + 2EtOH + H_2S	DA + H_2S	EtOH
H_2 production (μmol h^{-1})	1190	660	230	5

[a] DEA: diethanolamine, DA: diethylamine. Reaction conditions: volume of solution, 100 ml; concentration of H_2S, 0.30 M; amount of catalyst, 0.025 g; reaction temperature, 30 °C; light source, 300-W Xe lamp with a cutoff filter ($\lambda > 420$ nm).

To reclaim sulfur from the H_2S–DEA solution after photocatalytic reaction, hydrochloric acid (3 M) was added to the reacted solution. A light-yellow powder was separated from the solution when the pH value was below 6. XRD patterns (Fig. 2, inset) of the products reclaimed from the reaction solution clearly indicate that the solid product was mainly crystallized sulfur in orthorhombic phase. Table 2 gives the total amount of H_2 and S produced from the H_2S–DEA solution after photocatalytic reaction. For different runs of the reaction, the molar ratio of the H_2 and S produced was close to 1:1, meaning that H_2S was stoichiometrically split into H_2 and S. These results demonstrate that the direct splitting of H_2S into the elements S and H_2 ($H_2S \rightarrow S + H_2$) was realized by the photocatalytic reaction on M/CdS under visible light irradiation.

3.3. *Influence of hydroxyls on photocatalytic reaction*

The H_2 production activity was found to be much lower when the photocatalytic reaction was conducted in H_2S–diethylamine (H_2S–DA) solution than in H_2S–diethanolamine (H_2S–DEA) solution (Table 3). The big difference between DEA and DA is that DEA has hydroxyl groups and DA does not. Interestingly, a mixture of DA and ethanol gave much higher activity in H_2 production than DA alone (Table 3). Obviously, the hydroxyl groups of the solvent play an important role in the photocatalytic splitting of H_2S, and possibly the hydroxyl groups of the solvent promote proton transportation in the reaction, because a crucial step for photocatalytic hydrogen production is proton transfer, which may occur on the catalyst surface or/and through the reaction media. The hydroxyl groups in solution may possibly facilitate the transferring of protons from nonactive sites to active sites on CdS and from bulk solution to the CdS surface [26].

3.4. *Rate-determining step of the photocatalytic reaction*

The photocatalytic reduction of protons and oxidation of sulfide ions must proceed simultaneously to create a balance of electrons and holes on a semiconductor catalyst. It can be seen from Table 4 that the H_2 production rate was higher in 0.5 M H_2S–DEA than in 0.3 M H_2S–DEA. Adding 0.2 M H_2SO_4 to the 0.3 M H_2S–DEA solution to make a solution with the same number of protons as in the 0.5 M H_2S–DEA solution had no affect on the photocatalytic H_2 production rate; however, adding 0.2 M Na_2S to the 0.3 M H_2S–DEA solution to make a solution with the same number of sulfide ions as in the 0.5 M H_2S–DEA solution did improve the H_2 production rate. The photocatalytic performance was nearly the same in the 0.2 M Na_2S + 0.3 M H_2S–DEA and 0.5 M H_2S–DEA solutions. These results imply that the oxidation process is the RDS in the photocatalytic splitting of H_2S.

Table 4
Influence of different composition of reactants on H_2 production rate under visible light irradiation.

Composition of reactants	H_2 production (μmol h^{-1})
0.30 M H_2S	1190
0.30 M H_2S + 0.20 M H_2SO_4	1200
0.30 M H_2S + 0.20 M Na_2S	1410
0.50 M H_2S	1480

Reaction conditions: reaction solution, 100 ml DEA; catalyst, 0.025 g Pt (0.2 wt%)/CdS; reaction temperature, 30 °C; light source, 300-W Xe lamp with a cutoff filter ($\lambda > 420$ nm).

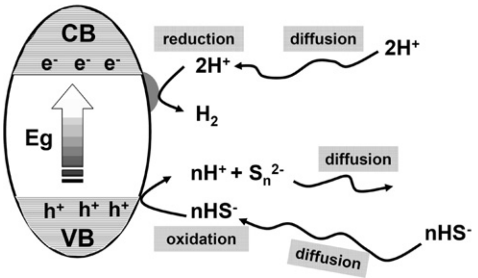

Scheme 1. Photocatalytic process of splitting H_2S in DEA.

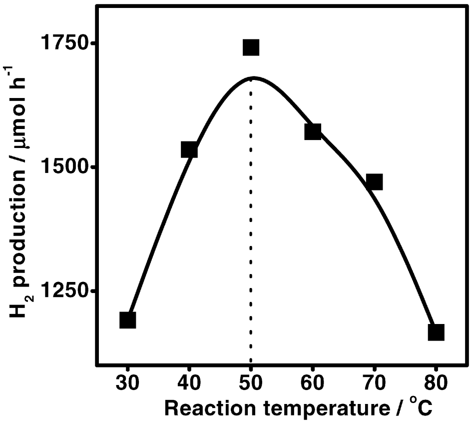

Fig. 4. Dependence of H_2 production rate upon reaction temperature under visible light irradiation. Reaction conditions: reaction solution, 100 ml DEA; concentration of H_2S, 0.30 M; catalyst, 0.025 g Pt (0.2 wt%)/CdS; light source, 300-W Xe lamp with a cutoff filter ($\lambda > 420$ nm).

As shown in Scheme 1, the oxidation process can be roughly divided into three steps: (1) diffusion of sulfide ions from bulk solution to the CdS surface, (2) photo-oxidation of sulfide ions to polysulfide ions by holes on CdS, and (3) diffusion of polysulfide ions from the CdS surface to bulk solution. Fig. 4 shows the influence of temperature on photocatalytic activity of splitting H_2S in a DEA solution. It can be seen that the H_2 production rate increases sharply with increasing reaction temperature from room temperature to about 50 °C. The drop in the H_2 production rate above 50 °C was likely due to the reaction between polysulfide (oxidant) and DEA (reductant) at high temperature. The viscosity of DEA solution and the diffusion rate of ions in DEA are highly temperature-dependent. Based on the dependence of H_2 production rate on reaction temperature, especially at temperatures below 50 °C, we assume that the diffusion of sulfide or polysulfide ions is the RDS.

Fig. 5 shows the dependence of the photocatalytic H_2 production rate on the H_2S concentration in the DEA solution. CdS loaded

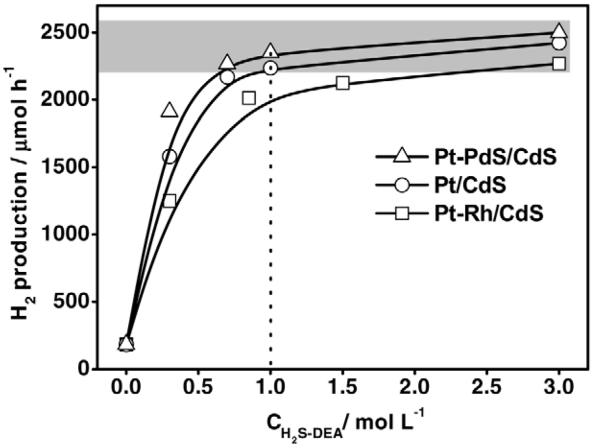

Fig. 5. Dependence of H_2 production rate under visible light irradiation upon H_2S concentration on Pt (0.2 wt%)/CdS, Pt–PdS (0.2–0.2 wt%)/CdS and Pt–Rh (0.2–0.2 wt%)/CdS. Reaction conditions: reaction solution, 100 ml DEA; amount of catalyst, 0.025 g; reaction temperature, 30 °C; light source, 300-W Xe lamp with a cutoff filter ($\lambda > 420$ nm).

Table 5
Instantaneous photocatalytic H_2 production rate under visible light irradiation over Pt (0.2 wt%)/CdS in non-aqueous DEA + H_2S and in aqueous NaOH + Na_2S solution.[a]

H_2 production rate (µmol h^{-1})	Reaction time (h)					
	1	2	3	4	5	6
DEA + H_2S	1250	1580	1010	1070	1040	1010
NaOH + H_2S	490	530	130	220	80	50

[a] Reaction conditions: volume of solution, 100 ml; concentration of H_2S, 0.30 M; amount of catalyst, 0.025 g; reaction temperature, 30 °C; light source, 300-W Xe lamp with a cutoff filter ($\lambda > 420$ nm).

with Pt, Pt–PdS, and Pt–Rh as photocatalysts were evaluated. The photocatalytic H_2 production rate was found to vary with different noble metals and to increase linearly with H_2S concentration at an H_2S concentration in DEA < 1 M. However, interestingly, the H_2 production rates appeared to level off near a similar value on CdS loaded with Pt, Pt–PdS, and Pt–Rh when the H_2S concentration was varied between 1 and 3 M. This implies that the activity of photocatalytic splitting of H_2S in DEA is not influenced by reactants but is influenced by products at a higher H_2S concentration. According to the assumption of RDS mentioned above, here we propose that the RDS of photocatalytic splitting of H_2S in DEA is the diffusion of polysulfide ions from CdS surface to bulk solution when the photocatalytic H_2 production rate reaches a constant. With such a proposal, we can explain the experimental results shown in Fig. 5—namely, the high production of polysulfide ions at high H_2S concentration cover the CdS surface, and the sulfide ions (even at high quantities) must "wait" for the diffusion of polysulfide ions to provide reaction sites. The quantum efficiency for H_2 production from photocatalytic splitting H_2S in DEA may be as high as 30% at 420 nm under optimal reaction conditions.

3.5. Comparison of photocatalytic H_2 production between Na_2S–NaOH and H_2S–DEA

As mentioned at the beginning of this paper, in basic aqueous solutions, the sulfide ions must be used together with sulfite ions as sacrificial agents for photocatalytic H_2 production. This is because that the sulfide ions alone show poor stability for H_2 production in an aqueous reaction system. Table 5 compares the photocatalytic H_2 production of a nonaqueous H_2S–DEA solution and an aqueous Na_2S–NaOH solution (H_2S dissolved in NaOH) on a Pt/CdS catalyst. It can be seen that both the activity and stability of hydrogen production were much higher in the H_2S–DEA solution than in the aqueous Na_2S–NaOH solution. After 6 h of reaction, the instantaneous H_2 production rate dropped from the starting value of 1250 µmol h^{-1} to 1010 µmol h^{-1} in the H_2S–DEA solution and from 490 µmol h^{-1} to 50 µmol h^{-1} in the aqueous Na_2S–NaOH solution. In basic solutions, polysulfide ions have strong absorption of UV and visible light [13,27,30,31]. In the H_2S–DEA solution, the pholysulfide ions produced during the course of photocatalytic reaction on M/CdS act as an optical filter reducing the light absorption of CdS. As shown in Table 5, the H_2 production rate decreased gradually as the reaction proceeded, with the accumulation of polysulfide ions in the DEA solution.

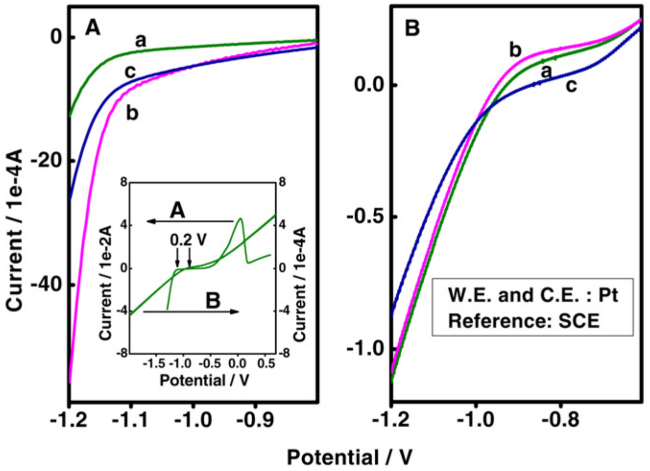

Fig. 6. Linear sweep voltammetry of (A) aqueous 0.3 M Na_2S + 1 M NaOH solution and (B) 0.3 M H_2S–DEA solution under a scan rate of 50 mV S^{-1} at room temperature with platinum patch as working and counter electrode and SCE as reference. The I–V curves are (a) fresh solution, (b) the solution of (a) containing polysulfide produced by in situ electrochemical oxidation of sulfide ions, (c) the solution of (a) after photocatalytic reaction. The inset shows the comparison of the linear sweep voltammetry of fresh solutions A and B.

3.6. Electrochemical evaluation

3.6.1. Electrochemical reduction of protons

To gain insight into the difference between nonaqueous H_2S–DEA and aqueous Na_2S–NaOH solutions, the reduction of protons on the Pt electrodes in the two solutions was investigated using an electrochemical linear sweep voltammetry method. Fig. 6 shows the reduction potential changes of the two solutions with and without polysulfide ions. We can see that the hydrogen evolution potential was about 0.20 V lower in the H_2S–DEA solution than in the Na_2S–NaOH aqueous solution. This means that protons were more readily reduced in DEA than in the aqueous Na_2S–NaOH solution. To evaluate the affect of polysulfide ions on the reduction of protons, the I–V curves were measured for the two solutions with equal amounts of polysulfide ions produced by in situ electrochemical oxidation of sulfide ions. The results, shown in Fig. 6, clearly show that addition of the polysulfide ions greatly increased the current at the same voltage in the aqueous Na_2S–NaOH solution, whereas no evident change in current occurred in the H_2S–DEA solution. The H_2S–DEA and Na_2S–NaOH solutions with polysulfide ions formed after the photocatalytic reactions also were investigated by the electrochemical method. The curves show a same trend in the two solutions (Fig. 6). The presence of polysulfide in the Na_2S–NaOH solution can increase the reductive current in electrochemistry, because the polysulfide ions can be reduced on the Pt electrodes. The electrochemical results for the Na_2S–NaOH solution can explain the poor stability for photocatalytic hydrogen production in this solution reported in the literature [13–15]. The consumption of photogenerated electrons on CdS photocatalyst

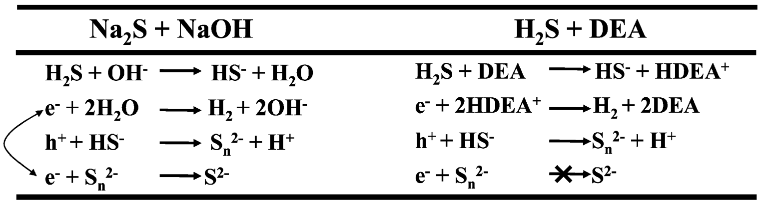

Scheme 2. Different photocatalytic processes of splitting H_2S in aqueous Na_2S + NaOH solution and in H_2S + DEA solution.

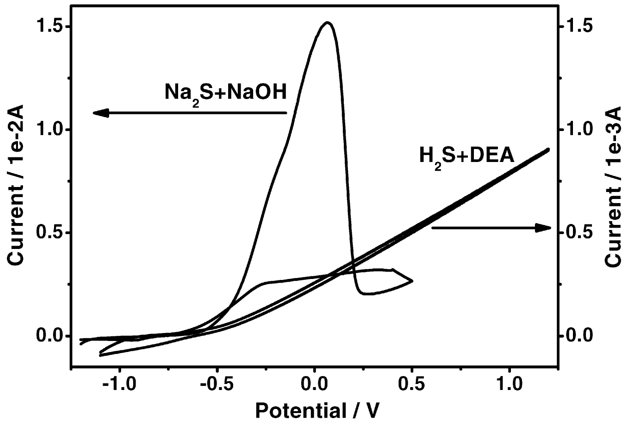

Fig. 7. Cyclic voltammetry of aqueous 0.3 M Na_2S + 1 M NaOH solution and 0.3 M H_2S–DEA solution under a scan rate of 50 $mV\,S^{-1}$ at room temperature with platinum patch as working and counter electrode and SCE as reference.

by polysulfide ions reduces the amount of electrons for hydrogen production. The similar electrochemical reductive current after the addition of polysulfide ions to the H_2S–DEA solution explains the relatively higher photocatalytic hydrogen production activity and stability in the H_2S–DEA solution compared with the aqueous Na_2S–NaOH solution (Table 5); in other words, the electron consumption reaction by polysulfide ions was depressed in the H_2S–DEA solution, and the photogenerated electrons on the CdS photocatalyst are involved mainly in hydrogen production. Scheme 2 summarizes the different photocatalytic processes involved in the splitting of H_2S in the aqueous Na_2S–NaOH and H_2S–DEA solutions.

3.6.2. Electrochemical oxidation of sulfide ions

Fig. 7 shows the electrochemical oxidation of sulfide ions in the aqueous Na_2S–NaOH and H_2S–DEA solutions on platinum electrodes. According to the literature [32,33], the anodic peak at 0.07 V in Na_2S–NaOH solution is due to the passivation of sulfur on platinum electrodes. Szynkarczuk et al. [33] even found that the HS^- ions were oxidized in two stages, (1) oxidation of the hydrosulfide ions into intermediate polysulfide ions and (2) the further oxidation to elemental sulfur:

$$n\mathrm{HS}^- + n\mathrm{OH}^- \rightarrow \mathrm{S}_n^{2-} + n\mathrm{H_2O} + 2(n-1)\mathrm{e}^-, \tag{1}$$

$$\mathrm{S}_n^{2-} \rightarrow n\mathrm{S}^0 + 2\mathrm{e}^-. \tag{2}$$

In the aqueous Na_2S–NaOH solution, a white film was deposited on the platinum electrode after several runs of electrochemical oxidation. In the H_2S–DEA solution, as shown in Fig. 7, the oxidation current increased linearly with increasing anodic potential, and no peak was observed even at a high potential value. The platinum electrodes remained clean during the oxidation of sulfide ions in the H_2S–DEA solution. This finding implies a different oxidation mechanism from sulfide ions to polysulfide ions in the H_2S–DEA solution than that in the aqueous Na_2S–NaOH solution. Here we propose a free-radical-related one-electron electrochemical oxidation process in the H_2S–DEA solution:

$$\mathrm{HS}^- \rightarrow \mathrm{HS}^{\bullet} + \mathrm{e}^-. \tag{3}$$

The mercapto radical ($HS^{\bullet}$) readily produces polysulfide ions (S_n^{2-}) or polysulfide radicals ($S_n^{\bullet-}$) by deprotonation and/or dimerization in basic H_2S–DEA solution [34], rather than producing solid sulfur film deposited on platinum electrodes.

The electrochemical oxidation of sulfide ions in aqueous solution using different electrodes, including Pt [32,33], Au [35], and graphite [36], has been reported previously. But the passivation of anode caused by sulfur deposition is inevitable, which seriously decreases the efficiency of electrochemical decomposition of H_2S. The possible development of DEA solution as a media for electrochemical oxidation of sulfide ions may overcome this disadvantage.

4. Conclusion

In summary, we found that H_2S can be directly split into hydrogen and sulfur on photocatalysts composed of CdS-based semiconductors loaded with noble metals and noble metal sulfides using nonaqueous ethanolamine solvent as the reaction media. The quantum efficiency in hydrogen production can be as high as 30% under visible light irradiation. DEA was found to be an excellent reaction media for this reaction, possibly because it is a suitable medium for proton transfer and also an effective solvent to keep polysulfide ions from consuming photogenerated electrons on the CdS photocatalysts. The diffusion of polysulfide ions from the CdS surface to bulk solution is proposed to be the RDS in the photocatalytic splitting of H_2S at high H_2S concentrations. Electrochemical analysis indicated that protons were more readily reduced in DEA than in the aqueous NaOH solution and that the splitting potential of H_2S was significantly lower in DEA than in the usually studied Na_2S–NaOH aqueous solution. The deposition of sulfur on electrodes during the electrochemical oxidation process was avoided in the H_2S–DEA solution, likely due to a free-radical-related one-electron oxidation mechanism. The development of a nonaqueous ethanolamine solution as a solvent and reaction medium provides a new strategy for the decomposition of H_2S by both photocatalytic and electrochemical technology.

Acknowledgments

This work was supported by the National Natural Science Foundation of China (grants 20503034 and 673112), the National Basic Research Program of China (grant 2003CB214504), the Knowledge Innovation Program of the Chinese Academy of Sciences, DICP (grant K2006E2), and the Programme for Strategic Scientific Alliances between China and the Netherlands (grant 2008KR0531).

References

[1] U.S. Department of Health and Human Services, Toxicological profile for hydrogen sulfide, CAS No. 123-91-1, 2006, p. 14; http://www.atsdr.cdc.gov/toxprofiles/tp114.pdf.
[2] R.G. Hendrickson, A. Chang, R. Hamilton, Am. J. Ind. Med. 45 (2004) 346.

[3] A.D.S. Gillies, H.W. Wu, M.S. Kizil, T. Harvey, The mining challenge of coal seam hydrogen sulfide, in: Proc. Queensland Min. Ind. Health Saf. Conf., Townsville, August 2000, p. 375.
[4] G. Etiope, G. Papatheodorou, D. Christodoulou, P. Favalil, G. Ferentinos, TAO 16 (2005) 897.
[5] J.A. Rodriguez, A. Maiti, J. Phys. Chem. B 104 (2000) 3630.
[6] M. Flytzoni-Stephanopoulos, M. Sakbodin, Zh. Wang, Science 312 (2006) 1508.
[7] A. Vrachnos, G. Kontogeorgis, E. Voutsas, Ind. Eng. Chem. Res. 45 (2006) 5148.
[8] I.A. Gargurevich, Ind. Eng. Chem. Res. 44 (2005) 7706.
[9] J. Zaman, A. Chakma, Fuel Process. Technol. 41 (1995) 159.
[10] M. Binoist, B. Labegorre, F. Monnet, P.D. Clark, N.I. Dowling, M. Huang, D. Archambault, E. Plasari, P.-M. Marquaire, Ind. Eng. Chem. Res. 42 (2003) 3943.
[11] K. Maeda, K. Teramura, D. Lu, T. Takata, N. Saito, Y. Inoue, K. Domen, Nature 440 (2006) 295.
[12] O. Morton, Nature 443 (2006) 19.
[13] J.-F. Reber, K. Meier, J. Phys. Chem. 88 (1984) 5903.
[14] N. Bühler, K. Meier, J.-F. Reber, J. Phys. Chem. 88 (1984) 3261.
[15] N. Bao, L. Shen, T. Takata, K. Domen, Chem. Mater. 20 (2008) 110.
[16] Z. Lei, W. You, M. Liu, G. Zhou, T. Takata, M. Hara, K. Domen, C. Li, Chem. Commun. (2003) 2142.
[17] I. Tsuji, H. Kato, A. Kudo, Angew. Chem. Int. Ed. 44 (2005) 3565.
[18] A. Ishikawa, T. Takata, J.N. Kondo, M. Hara, H. Kobayashi, K. Domen, J. Am. Chem. Soc. 124 (2002) 13547.
[19] M. Liu, W. You, Z. Lei, G. Zhou, J. Yang, G. Wu, G. Ma, G. Luan, T. Takata, M. Hara, K. Domen, C. Li, Chem. Commun. (2004) 2192.
[20] F.-Y. Jou, F.D. Otto, A.E. Mather, J. Chem. Eng. Data 41 (1996) 1181.
[21] E.B. Bouhelec, P. Mogin, A. Barreau, R. Solimando, Energy Fuels 21 (2007) 2044.
[22] S.A. Naman, M. Grätzel, J. Photochem. Photobiol. A: Chem. 77 (1994) 249.
[23] S.A. Naman, N.H. Al-Mishhadani, L.M. Al-Shamma, Int. J. Hydrogen Energy 20 (1995) 303.
[24] M. Green, R.M. Elofson, Chem. Commun. (1985) 830.
[25] A.L. Linsebigler, G. Lu, J.T. Yates, Chem. Rev. 95 (1995) 735.
[26] T. Chen, Z. Feng, G. Wu, G. Ma, P. Ying, C. Li, J. Phys. Chem. C 111 (2007) 8005.
[27] P. Dubois, J.P. Lelieur, G. Lepoutre, Inorg. Chem. 27 (1988) 1883.
[28] R. Steudel, Top. Curr. Chem. 231 (2003) 99.
[29] R. Steudel, Top. Curr. Chem. 231 (2003) 127.
[30] P. Dubois, J.P. Lelieur, G. Lepoutre, Inorg. Chem. 26 (1987) 1897.
[31] T. Chivers, I. Drummond, Inorg. Chem. 11 (1972) 2525.
[32] S. Kapusta, A. Viehbeck, S.M. Wilhelm, N. Hackerman, J. Electroanal. Chem. 153 (1983) 157.
[33] J. Szynkarczuk, P.G. Komorowski, J.C. Donini, Electrochim. Acta 39 (1994) 2285.
[34] R. Steudel, Ind. Eng. Chem. Res. 35 (1996) 1417.
[35] A. Briceno, S. Chander, J. Appl. Electrochem. 20 (1990) 512.
[36] Z. Mao, A. Anani, R.E. White, S. Srinivasan, A.J. Appleby, J. Electrochem. Soc. 138 (1991) 1299.